Observation of Five New Narrow Ω[superscript 0]c States Decaying to ##cK#

Observation of Five New Narrow Ω_c^0 States Decaying to $\Xi_c^+ K^-$

R. Aaij *et al.*[*]
(LHCb Collaboration)

(Received 14 March 2017; published 2 May 2017)

The $\Xi_c^+ K^-$ mass spectrum is studied with a sample of pp collision data corresponding to an integrated luminosity of 3.3 fb^{-1}, collected by the LHCb experiment. The Ξ_c^+ is reconstructed in the decay mode $pK^-\pi^+$. Five new, narrow excited Ω_c^0 states are observed: the $\Omega_c(3000)^0$, $\Omega_c(3050)^0$, $\Omega_c(3066)^0$, $\Omega_c(3090)^0$, and $\Omega_c(3119)^0$. Measurements of their masses and widths are reported.

DOI: 10.1103/PhysRevLett.118.182001

The spectroscopy of singly charmed baryons cqq' is intricate. With three quarks and numerous degrees of freedom, many states are expected. At the same time, the large mass difference between the charm quark and the light quarks provides a natural way to understand the spectrum by using the symmetries provided by the heavy quark effective theory (HQET) [1,2]. In recent years, considerable improvements have been made in the predictions of the properties of these heavy baryons [3–14]. In many of these models, the heavy quark interacts with a (qq') diquark, which is treated as a single object. These models predict seven states in the mass range 2.9–3.2 GeV (natural units are used throughout this Letter), some of them narrow. Other models make use of lattice QCD calculations [15].

The spectroscopy of charmed baryons, particularly the Λ_c^+, Σ_c, and Ξ_c states, has also seen considerable experimental progress, with results obtained at the B factories and is in the physics program of the LHCb experiment at CERN [16,17]. Among the expected charmed baryon states, this work addresses the Ω_c^0 baryons, which have quark content css and isospin zero. Their spectrum is largely unknown: Only the Ω_c^0 and $\Omega_c(2770)^0$, presumed to be the $J^P = 1/2^+$ and $3/2^+$ ground states, have been observed [16,18].

To improve the understanding of this little-explored sector of the charmed baryon spectrum, this Letter presents a search for new Ω_c^0 resonances that decay strongly to the final state $\Xi_c^+ K^-$, where the Ξ_c^+ is a weakly decaying charmed baryon with quark content csu. (The inclusion of charge-conjugate processes is implied throughout, unless stated otherwise.) The measurement is based on samples of pp collision data corresponding to integrated luminosities of 1.0, 2.0, and 0.3 fb^{-1} at center-of-mass energies of 7, 8, and 13 TeV, respectively, recorded by the LHCb experiment. The LHCb detector is a single-arm forward spectrometer covering the pseudorapidity range $2 < \eta < 5$, designed for the study of particles containing b or c quarks, and is described in detail in Refs. [19,20]. Hadron identification is provided by two ring-imaging Cherenkov detectors [21], a calorimeter system, and a muon detector. The online event selection is performed by a trigger, which consists of a hardware stage, based on information from the calorimeter and muon systems, followed by a software stage, which applies a full event reconstruction [22]. Simulated events are produced with the software packages described in Refs. [23–28].

The reconstruction begins with the Ξ_c^+ baryon, via the decay $\Xi_c^+ \to pK^-\pi^+$. The Ξ_c^+ candidates are formed from combinations of three tracks that originate from a common vertex. These are required to pass a cut-based preselection and then a multivariate selection based on likelihood ratios, described below. Candidates fulfilling these requirements are then combined with a fourth track to form $\Omega_c^0 \to \Xi_c^+ K^-$ candidates to which additional selection requirements, also described below, are applied.

The Ξ_c^+ preselection requires a positively identified proton and a large Ξ_c^+ flight-distance significance (defined as the measured flight distance divided by its uncertainty) from a primary pp interaction vertex (PV). The Ξ_c^+ candidates are also constrained to originate from the PV by requiring a small $\chi^2_{\rm IP}$ (defined as the difference between the vertex fit χ^2 of the PV reconstructed with and without the candidate in question). The resulting $pK^-\pi^+$ mass spectrum is fitted with a linear function to describe the background and the sum of two Gaussian functions with a common mean to describe the signal. The fit is used to define signal and sideband regions of the Ξ_c^+ invariant mass spectrum: The signal region consists of the range within $\pm 2.0\sigma$ of the fitted mass, where $\sigma = 6.8$ MeV is the weighted average of the standard deviations of the Gaussian functions, and the sidebands cover the range $3.5 - 5.5\sigma$ on either side. The fit is also used to determine the Ξ_c^+ purity after the preselection, defined as the signal

[*]Full author list given at the end of the article.

yield in the signal region divided by the total yield in the same region. A purity of 41% is obtained, which is not sufficient for the spectroscopy study but allows the extraction of background-subtracted probability density functions (PDFs) of the kinematic and geometric properties of the signal. These distributions are taken from the data rather than the simulation, given the limited understanding of heavy baryon production dynamics and the difficulty of modeling them correctly for different center-of-mass energies.

For each variable of interest, the background PDF is obtained from the corresponding distribution in the mass sideband regions and is also used for the background subtraction. The signal PDF is obtained from the normalized, background-subtracted distribution in the signal mass region. Variables found to have a good discrimination between the signal and background are the vertex fit χ^2, the Ξ_c^+ flight-distance significance and $\chi^2_{\rm IP}$, the particle identification probability for the proton and the kaon from the Ξ_c^+ decay, the $\chi^2_{\rm IP}$ of the three individual tracks, the Ξ_c^+ transverse momentum p_T with respect to the beam axis, the pseudorapidity η, and the angle between the Ξ_c^+ momentum and the vector joining the PV and the Ξ_c^+ decay vertex.

The PDFs of the 11 variables ($\mathbf{x}$) above are used to form a likelihood ratio, whose logarithm is defined as

$$\mathcal{L}(\mathbf{x}) = \sum_{i=1}^{11} [\ln \mathrm{PDF}_{\rm sig}(x_i) - \ln \mathrm{PDF}_{\rm back}(x_i)], \qquad (1)$$

where $\mathrm{PDF}_{\rm sig}$ and $\mathrm{PDF}_{\rm back}$ are the PDF distributions for the signal and background, respectively. Correlations between the variables are neglected in the likelihood.

The likelihood ratios and their PDFs are defined separately for the three data sets at different center-of-mass energies due to their different trigger conditions. The selection requirements on the likelihood ratios are also chosen separately for the three samples and lead to Ξ_c^+ purities of approximately 83% in the inclusive Ξ_c^+ sample.

Figure 1 shows the $pK^-\pi^+$ mass spectrum of Ξ_c^+ candidates passing the likelihood ratio selection for all three data sets combined, along with the result of a fit with the functional form described above. The Ξ_c^+ signal region contains 1.05×10^6 events. Note that this inclusive Ξ_c^+ sample contains not only those produced in the decays of charmed baryon resonances but also from other sources, including decays of b hadrons and direct production at the PV.

Each Ξ_c^+ candidate passing the likelihood ratio selection and lying within the Ξ_c^+ signal mass region is then combined in turn with each K^- candidate in the event. A vertex fit is used to reconstruct each $\Xi_c^+ K^-$ combination, with the constraint that it originates from the PV. The $\Xi_c^+ K^-$ candidate must have a small vertex fit χ^2, a high kaon identification probability, and transverse momentum $p_T(\Xi_c^+ K^-) > 4.5$ GeV.

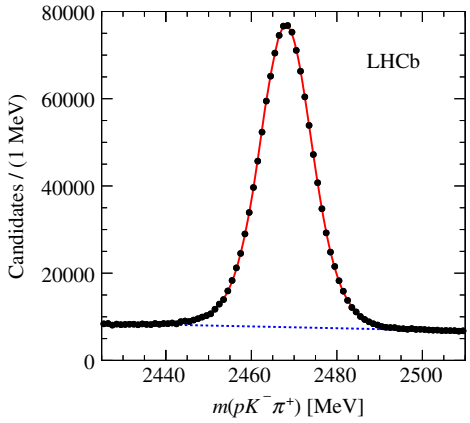

FIG. 1. Distribution of the reconstructed invariant mass $m(pK^-\pi^+)$ for all candidates in the inclusive Ξ_c^+ sample passing the likelihood ratio selection described in the text. The solid (red) curve shows the result of the fit, and the dashed (blue) line indicates the fitted background.

The $\Xi_c^+ K^-$ invariant mass is computed as

$$m(\Xi_c^+ K^-) = m([pK^-\pi^+]_{\Xi_c^+} K^-) - m([pK^-\pi^+]_{\Xi_c^+}) + m_{\Xi_c^+}, \qquad (2)$$

where $m_{\Xi_c^+} = 2467.89^{+0.34}_{-0.50}$ MeV is the world-average Ξ_c^+ mass [16] and $[pK^-\pi^+]_{\Xi_c^+}$ is the reconstructed $\Xi_c^+ \to pK^-\pi^+$ candidate.

In this analysis, the distribution of the invariant mass $m(\Xi_c^+ K^-)$ is studied from the threshold up to 3450 MeV.

The $\Xi_c^+ K^-$ mass distribution for the combined data sets is shown in Fig. 2, where five narrow structures are observed. To investigate the origin of these structures,

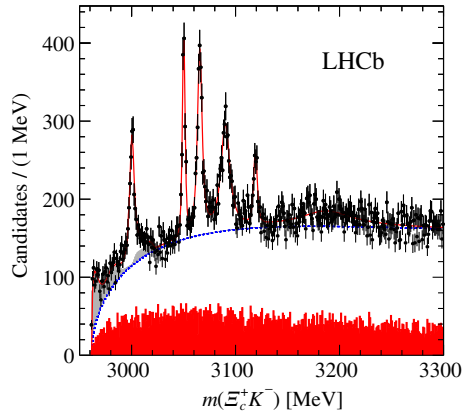

FIG. 2. Distribution of the reconstructed invariant mass $m(\Xi_c^+ K^-)$ for all candidates passing the likelihood ratio selection; the solid (red) curve shows the result of the fit, and the dashed (blue) line indicates the fitted background. The shaded (red) histogram shows the corresponding mass spectrum from the Ξ_c^+ sidebands, and the shaded (light gray) distributions indicate the feed-down from partially reconstructed $\Omega_c(X)^0$ resonances.

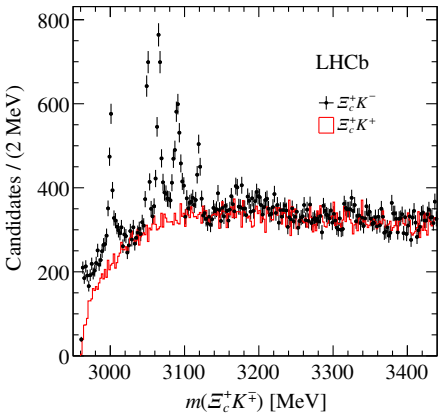

FIG. 3. Distribution of the reconstructed invariant mass $m(\Xi_c^+K^-)$ for all candidates passing the likelihood ratio selection, shown as black points with error bars, and the wrong-sign $m(\Xi_c^+K^+)$ spectrum scaled by a factor of 0.95, shown as a solid (red) histogram.

Fig. 2 also shows the distribution of $m(\Xi_c^+K^-)$ in the Ξ_c^+ sidebands as a shaded (red) histogram; no structure is seen in this background sample. In addition, wrong-sign $\Xi_c^+K^+$ combinations are processed in the same way as the right-sign combinations. The resulting wrong-sign $\Xi_c^+K^+$ mass spectrum is shown in Fig. 3, scaled by a factor of 0.95 so that the two spectra approximately match at a large invariant mass, along with the right-sign $m(\Xi_c^+K^-)$ spectrum for comparison. No structure is observed in the wrong-sign mass spectrum. The absence of corresponding features in the control samples is consistent with the five structures being resonant states, henceforth denoted $\Omega_c(X)^0$ for mass X. It can also be seen that the two mass spectra in Fig. 3 exhibit different behavior close to the $\Xi_c^+K^-$ threshold (2960–2970 MeV). The right-sign distribution has a much steeper rise compared to the wrong-sign spectrum, suggesting the presence of additional components in the $\Xi_c^+K^-$ mass spectrum as discussed below.

Further tests are performed by studying combinations of one of the $\Xi_c^+ \to pK^-\pi^+$ decay products with the other kaon used to form the $\Omega_c(X)^0$ candidate (i.e., pK^-, K^-K^-, and π^+K^-). The resulting two-body invariant mass spectra do not show any structure except for a small $\bar{K}^{*0}$ signal in the π^+K^- mass, also visible in the Ξ_c^+ sidebands, which is attributed to background contributions. Another class of potential misreconstruction consists of $\Xi_c^+\pi^-$ combinations in which the π^- is misidentified as a kaon. To test for this, the selected $\Xi_c^+K^-$ sample is investigated with the pion mass assigned to the kaon candidate. No narrow peaks are observed in this pseudo-$\Xi_c^+\pi^-$ spectrum, indicating that peaks in the $\Xi_c^+K^-$ spectrum do not arise from misidentified $\Xi_c^+\pi^-$ resonances.

The wrong-sign $\Xi_c^+K^+$ sample is used to study the combinatorial background. The parameterization used is [29]

$$B(m) = \begin{cases} P(m)e^{a_1 m + a_2 m^2} & \text{for } m < m_0, \\ P(m)e^{b_0 + b_1 m + b_2 m^2} & \text{for } m > m_0, \end{cases} \quad (3)$$

where $P(m)$ is a two-body phase-space factor and m_0, a_i, and b_i are free parameters. Both $B(m)$ and its first derivative must be continuous at $m = m_0$; these constraints reduce the number of free parameters to four. This model gives a good description of the wrong-sign mass spectrum up to a mass of 3450 MeV with a p value of 18% for a binned χ^2 fit.

To study the reconstruction efficiency and the mass resolution of each of the structures, samples of simulated events are generated in which $\Omega_c(X)^0$ resonances decay to $\Xi_c^+K^-$, with the masses and natural widths of the $\Omega_c(X)^0$ chosen to approximately match those seen in the data. The mass residuals, defined as the difference between the generated $\Omega_c(X)^0$ mass and the reconstructed value of $m(\Xi_c^+K^-)$, are well described by the sum of two Gaussian functions with a common mean. The parameters of these fits are used to determine the mass-dependent experimental resolution, which runs from 0.75 MeV at 3000 MeV to 1.74 MeV at 3119 MeV, and is found to be well described by a linear function. The simulation samples are also used to obtain the reconstruction efficiency, which is consistent with being constant as a function of $m(\Xi_c^+K^-)$.

Another possible decay mode for $\Omega_c(X)^0$ resonances is

$$\Omega_c(X)^0 \to K^-\Xi_c'^+ \quad \text{with} \quad \Xi_c'^+ \to \Xi_c^+\gamma \quad (4)$$

or, in general, to a final state that includes $\Xi_c^+K^-$ but also contains one or more additional particles that are not included in the reconstruction. For the case of a narrow $\Omega_c(X)^0$ resonance decaying via $\Xi_c'^+$, the resulting distribution in $m(\Xi_c^+K^-)$ is a relatively narrow structure that is shifted down in mass (feed-down) that needs to be taken into account in the description of the data. Simulation studies of the decay chain shown in Eq. (4) have been performed with resonance masses of 3066, 3090, and 3119 MeV. It is found that the feed-down shapes deviate from Breit-Wigner distributions and are therefore parameterized by B splines [30].

A binned χ^2 fit to the $m(\Xi_c^+K^-)$ spectrum is performed in the range from the threshold to 3450 MeV. In this fit, the background is modeled by Eq. (3), while the resonances are described by spin-zero relativistic Breit-Wigner functions convolved with the experimental resolution. In addition, three feed-down contributions arising from the partially reconstructed decays of $\Omega_c(3066)^0$, $\Omega_c(3090)^0$, and $\Omega_c(3119)^0$ resonances are included with fixed shapes but free yields. It is found that the fit improves if an additional broad Breit-Wigner function is included in the 3188 MeV mass region. This broad structure may be due to a single resonance, to the superposition of several resonances, to feed-down from higher states, or to some

TABLE I. Results of the fit to $m(\Xi_c^+ K^-)$ for the mass, width, yield, and significance for each resonance. The subscript fd indicates the feed-down contributions described in the text. For each fitted parameter, the first uncertainty is statistical and the second systematic. The asymmetric uncertainty on the $\Omega_c(X)^0$ arising from the Ξ_c^+ mass is given separately. Upper limits are also given for the resonances $\Omega_c(3050)^0$ and $\Omega_c(3119)^0$ for which the width is not significant.

Resonance	Mass (MeV)	Γ (MeV)	Yield	N_σ
$\Omega_c(3000)^0$	$3000.4 \pm 0.2 \pm 0.1^{+0.3}_{-0.5}$	$4.5 \pm 0.6 \pm 0.3$	$1300 \pm 100 \pm 80$	20.4
$\Omega_c(3050)^0$	$3050.2 \pm 0.1 \pm 0.1^{+0.3}_{-0.5}$	$0.8 \pm 0.2 \pm 0.1$	$970 \pm 60 \pm 20$	20.4
		<1.2 MeV, 95% C.L.		
$\Omega_c(3066)^0$	$3065.6 \pm 0.1 \pm 0.3^{+0.3}_{-0.5}$	$3.5 \pm 0.4 \pm 0.2$	$1740 \pm 100 \pm 50$	23.9
$\Omega_c(3090)^0$	$3090.2 \pm 0.3 \pm 0.5^{+0.3}_{-0.5}$	$8.7 \pm 1.0 \pm 0.8$	$2000 \pm 140 \pm 130$	21.1
$\Omega_c(3119)^0$	$3119.1 \pm 0.3 \pm 0.9^{+0.3}_{-0.5}$	$1.1 \pm 0.8 \pm 0.4$	$480 \pm 70 \pm 30$	10.4
		<2.6 MeV, 95% C.L.		
$\Omega_c(3188)^0$	$3188 \pm 5 \pm 13$	$60 \pm 15 \pm 11$	$1670 \pm 450 \pm 360$	
$\Omega_c(3066)^0_{\rm fd}$			$700 \pm 40 \pm 140$	
$\Omega_c(3090)^0_{\rm fd}$			$220 \pm 60 \pm 90$	
$\Omega_c(3119)^0_{\rm fd}$			$190 \pm 70 \pm 20$	

combination of the above. Under the simplest hypothesis, namely, that it is due to a single state, its parameters are given in Table I.

This configuration is denoted the reference fit and is shown in Fig. 2. No significant structure is seen above 3300 MeV. Table I gives the fitted parameters and yields of the resonances, along with the yields for the feed-down contributions indicated with the subscript "fd". The statistical significance of each resonance is computed as $N_\sigma = \sqrt{\Delta\chi^2}$, where $\Delta\chi^2$ is the increase in χ^2 when the resonance is excluded in the fit. Very high significances are obtained for all the narrow resonances observed in the mass spectrum. The threshold enhancement below 2970 MeV is fully explained by feed-down from the $\Omega_c(3066)^0$ resonance.

Several additional checks are performed to verify the presence of the signals and the stability of the fitted parameters. The likelihood ratio requirements are varied, testing both looser and tighter selections. As another test, the data are divided into subsamples according to the data-taking conditions, and each subsample is analyzed and fitted separately. The charge combinations $\bar{\Xi}_c^- K^+$ and $\Xi_c^+ K^-$ are also studied separately. In all cases, the fitted resonance parameters are consistent among the subsamples and with the results from the reference fit.

Systematic uncertainties on the Ω_c^0 resonance parameters are evaluated as follows. The fit bias is evaluated by generating and fitting an ensemble of 500 random mass spectra that are generated according to the reference fit. For each parameter, the absolute value of the difference between the input value and the mean fitted value of the ensemble is taken as the systematic uncertainty.

The background model uncertainty is estimated by exchanging it for the alternative function $B'(m) = (m - m_{\rm th})^\alpha e^{\beta+\gamma m+\delta m^2}$, where $m_{\rm th}$ is the threshold mass and α, β, γ, and δ are free parameters. The uncertainty associated with the choice of the Breit-Wigner model is estimated by fitting the data with relativistic $L = 1$, 2 Breit-Wigner functions with varying Blatt-Weisskopf factors [31] and is found to be negligible.

Resonances can interfere if they are close in mass and have the same spin parity. The effect is studied by introducing interference terms between each resonance and its neighboring resonances, one pair of resonances at a time. This is implemented with an amplitude of the form $A = |c_i \mathrm{BW}_i + c_j \mathrm{BW}_j e^{i\phi}|^2$ for the interference between resonances i and j, where BW_i and BW_j are complex Breit-Wigner functions and $c_{i,j}$ and ϕ are free parameters. For the central three resonances, where interference could occur with the state to the left or to the right, the absolute values of the deviations are added in quadrature. No evidence for interference effects is observed.

Recently, the Belle Collaboration has reported a measurement of the $\Xi_c'^+$ mass [32] that is significantly more precise than the previous value and which differs from it by +2.8 MeV. The effect of this is tested by shifting the $\Omega_c(3066)^0$, $\Omega_c(3090)^0$, and $\Omega_c(3119)^0$ feed-down shapes accordingly, and it is included as a systematic uncertainty.

The mass scale uncertainty is studied with a series of control samples and is found to be 0.03% of the mass difference from the threshold $(m - m_{\rm th})$. A comparison between the fitted Ξ_c^+ mass resolution in the data and simulation shows a 1.7% discrepancy, which is assigned as a systematic uncertainty on the width of the resonances. The description of the broad, high-mass structure labeled $\Omega_c(3188)^0$ is changed to the sum of four incoherent Breit-Wigner functions, and the effect on the other five resonances is included in the list of the systematic uncertainties. The largest contribution is found to be from possible interference, while the feed-down shift has a sizable effect only on the $\Omega_c(3000)^0$ parameters. For the

total systematic uncertainty, the individual contributions are added in quadrature. Finally, an uncertainty arises from the uncertainty on the Ξ_c^+ mass, whose world-average value is $m(\Xi_c^+) = 2467.89^{+0.34}_{-0.50}$ MeV [16]. It is quoted separately from the other uncertainties on the resonance masses and is the dominant uncertainty on several of them.

The $\Omega_c(3050)^0$ and $\Omega_c(3119)^0$ resonances have very narrow widths. For these states, Table I also includes Bayesian 95% confidence level (C.L.) upper limits [16] on the widths, evaluated from the statistical and systematic uncertainties assuming Gaussian PDFs.

The observation of these Ω_c states in an inclusive process through a two-body decay does not allow the determination of their quantum numbers, and therefore no attempt is made to compare the measured masses with HQET expectations. More information can be obtained from the study of possible three-body decays or when reconstructing these states in decays of heavy baryons.

In conclusion, the $\Xi_c^+ K^-$ mass spectrum is investigated using a data set corresponding to an integrated luminosity of 3.3 fb^{-1} collected by the LHCb experiment. A large and high-purity sample of Ξ_c^+ baryons is reconstructed in the Cabibbo-suppressed decay mode $pK^-\pi^+$. Five new, narrow excited Ω_c^0 states are observed: the $\Omega_c(3000)^0$, $\Omega_c(3050)^0$, $\Omega_c(3066)^0$, $\Omega_c(3090)^0$, and $\Omega_c(3119)^0$, and measurements of their masses and widths are reported. The data indicate also the presence of a broad structure around 3188 MeV that is fitted as a single resonance but could be produced in other ways, for example, as a superposition of several states. In addition, the partially reconstructed decay $\Omega_c(3066)^0 \to \Xi_c'^+ K^-$ is observed via its feed-down in the threshold region. Similarly, indications are found of $\Omega_c(3090)^0$ and $\Omega_c(3119)^0$ decays to $\Xi_c'^+ K^-$.

We express our gratitude to our colleagues in the CERN accelerator departments for the excellent performance of the LHC. We thank the technical and administrative staff at the LHCb institutes. We acknowledge support from CERN and from the national agencies: CAPES, CNPq, FAPERJ, and FINEP (Brazil); MOST and NSFC (China); CNRS/IN2P3 (France); BMBF, DFG, and MPG (Germany); INFN (Italy); NWO (The Netherlands); MNiSW and NCN (Poland); MEN/IFA (Romania); MinES and FASO (Russia); MinECo (Spain); SNSF and SER (Switzerland); NASU (Ukraine); STFC (United Kingdom); and NSF (USA). We acknowledge the computing resources that are provided by CERN, IN2P3 (France), KIT and DESY (Germany), INFN (Italy), SURF (The Netherlands), PIC (Spain), GridPP (United Kingdom), RRCKI and Yandex LLC (Russia), CSCS (Switzerland), IFIN-HH (Romania), CBPF (Brazil), PL-GRID (Poland), and OSC (USA). We are indebted to the communities behind the multiple open source software packages on which we depend. Individual groups or members have received support from AvH Foundation (Germany), EPLANET, Marie Skłodowska-Curie Actions, and ERC (European Union), Conseil Général de Haute-Savoie, Labex ENIGMASS, and OCEVU, Région Auvergne (France), RFBR and Yandex LLC (Russia), GVA, XuntaGal, and GENCAT (Spain), Herchel Smith Fund, The Royal Society, Royal Commission for the Exhibition of 1851, and the Leverhulme Trust (United Kingdom).

[1] A. G. Grozin, Introduction to the heavy quark effective theory. Part 1, arXiv:hep-ph/9908366.
[2] T. Mannel, Effective theory for heavy quarks, Lect. Notes Phys. **479**, 387 (1997).
[3] D. Ebert, R. N. Faustov, and V. O. Galkin, Masses of excited heavy baryons in the relativistic quark-diquark picture, Phys. Lett. B **659**, 612 (2008).
[4] W. Roberts and M. Pervin, Heavy baryons in a quark model, Int. J. Mod. Phys. A **23**, 2817 (2008).
[5] H. Garcilazo, J. Vijande, and A. Valcarce, Faddeev study of heavy-baryon spectroscopy, J. Phys. G **34**, 961 (2007).
[6] S. Migura, D. Merten, B. Metsch, and H.-R. Petry, Charmed baryons in a relativistic quark model, Eur. Phys. J. A **28**, 41 (2006).
[7] D. Ebert, R. N. Faustov, and V. O. Galkin, Spectroscopy and Regge trajectories of heavy baryons in the relativistic quark-diquark picture, Phys. Rev. D **84**, 014025 (2011).
[8] A. Valcarce, H. Garcilazo, and J. Vijande, Towards an understanding of heavy baryon spectroscopy, Eur. Phys. J. A **37**, 217 (2008).
[9] Z. Shah, K. Thakkar, A. K. Rai, and P. C. Vinodkumar, Mass spectra and Regge trajectories of Λ_c^+, Σ_c^0, Ξ_c^0 and Ω_c^0 baryons, Chin. Phys. C **40**, 123102 (2016).
[10] J. Vijande, A. Valcarce, T. F. Carames, and H. Garcilazo, Heavy hadron spectroscopy: A quark model perspective, Int. J. Mod. Phys. E **22**, 1330011 (2013).
[11] T. Yoshida, E. Hiyama, A. Hosaka, M. Oka, and K. Sadato, Spectrum of heavy baryons in the quark model, Phys. Rev. D **92**, 114029 (2015).
[12] H.-X. Chen, W. Chen, Q. Mao, A. Hosaka, X. Liu, and S. L. Zhu, P-wave charmed baryons from QCD sum rules, Phys. Rev. D **91**, 054034 (2015).
[13] H.-X. Chen, Q. Mao, A. Hosaka, X. Liu, and S. L. Zhu, D-wave charmed and bottomed baryons from QCD sum rules, Phys. Rev. D **94**, 114016 (2016).
[14] G. Chiladze and A. F. Falk, Phenomenology of new baryons with charm and strangeness, Phys. Rev. D **56**, R6738 (1997).
[15] M. Padmanath, R. G. Edwards, N. Mathur, and M. Peardon, Excited-state spectroscopy of singly, doubly and triply-charmed baryons from lattice QCD, arXiv:1311.4806.
[16] C. Patrignani *et al.* (Particle Data Group), Review of particle physics, Chin. Phys. C **40**, 100001 (2016).
[17] R. Aaij *et al.* (LHCb Collaboration), Search for the doubly charmed baryon Ξ_{cc}^+, J. High Energy Phys. 12 (2013) 090.
[18] E. Solovieva *et al.*, Study of Ω_c^0 and Ω_c^{*0} baryons at Belle, Phys. Lett. B **672**, 1 (2009).
[19] A. A. Alves, Jr. *et al.* (LHCb Collaboration), The LHCb detector at the LHC, J. Instrum. **3**, S08005 (2008).
[20] R. Aaij *et al.* (LHCb Collaboration), LHCb detector performance, Int. J. Mod. Phys. A **30**, 1530022 (2015).

[21] M. Adinolfi *et al.*, Performance of the LHCb RICH detector at the LHC, Eur. Phys. J. C **73**, 2431 (2013).
[22] R. Aaij *et al.*, The LHCb trigger and its performance in 2011, J. Instrum. **8**, P04022 (2013).
[23] T. Sjöstrand, S. Mrenna, and P. Skands, PYTHIA 6.4 physics and manual, J. High Energy Phys. 05 (2006) 026.
[24] I. Belyaev *et al.* (LHCb Collaboration), Handling of the generation of primary events in Gauss, the LHCb simulation framework, J. Phys. Conf. Ser. **331**, 032047 (2011).
[25] D. J. Lange, The EvtGen particle decay simulation package, Nucl. Instrum. Methods Phys. Res., Sect. A **462**, 152 (2001).
[26] P. Golonka and Z. Was, PHOTOS Monte Carlo: A precision tool for QED corrections in Z and W decays, Eur. Phys. J. C **45**, 97 (2006).
[27] S. Agostinelli *et al.* (Geant4 Collaboration), Geant4: A simulation toolkit, Nucl. Instrum. Methods Phys. Res., Sect. A **506**, 250 (2003); J. Allison *et al.* (Geant4 Collaboration), Geant4 developments and applications, IEEE Trans. Nucl. Sci. **53**, 270 (2006).
[28] M. Clemencic, G. Corti, S. Easo, C. R. Jones, S. Miglioranzi, M. Pappagallo, and P. Robbe (LHCb Collaboration), The LHCb simulation application, Gauss: Design, evolution and experience, J. Phys. Conf. Ser. **331**, 032023 (2011).
[29] P. del Amo Sanchez *et al.* (*BABAR* Collaboration), Observation of new resonances decaying to $D\pi$ and $D^*\pi$ in inclusive e^+e^- collisions near $\sqrt{s} = 10.58$ GeV, Phys. Rev. D **82**, 111101 (2010).
[30] C. De Boor, *A Practical Guide to Splines*, revised ed. (Springer, New York, 2001).
[31] J. Blatt and V. E. Weisskopf, *Theoretical Nuclear Physics* (Wiley, New York, 1952).
[32] J. Yelton *et al.* (Belle Collaboration), Study of excited Ξ_c states decaying into Ξ_c^0 and Ξ_c^+ baryons, Phys. Rev. D **94**, 052011 (2016).

R. Aaij,[40] B. Adeva,[39] M. Adinolfi,[48] Z. Ajaltouni,[5] S. Akar,[59] J. Albrecht,[10] F. Alessio,[40] M. Alexander,[53] S. Ali,[43] G. Alkhazov,[31] P. Alvarez Cartelle,[55] A. A. Alves Jr.,[59] S. Amato,[2] S. Amerio,[23] Y. Amhis,[7] L. An,[3] L. Anderlini,[18] G. Andreassi,[41] M. Andreotti,[17,a] J. E. Andrews,[60] R. B. Appleby,[56] F. Archilli,[43] P. d'Argent,[12] J. Arnau Romeu,[6] A. Artamonov,[37] M. Artuso,[61] E. Aslanides,[6] G. Auriemma,[26] M. Baalouch,[5] I. Babuschkin,[56] S. Bachmann,[12] J. J. Back,[50] A. Badalov,[38] C. Baesso,[62] S. Baker,[55] V. Balagura,[7,b] W. Baldini,[17] A. Baranov,[35] R. J. Barlow,[56] C. Barschel,[40] S. Barsuk,[7] W. Barter,[56] F. Baryshnikov,[32] M. Baszczyk,[27,c] V. Batozskaya,[29] B. Batsukh,[61] V. Battista,[41] A. Bay,[41] L. Beaucourt,[4] J. Beddow,[53] F. Bedeschi,[24] I. Bediaga,[1] A. Beiter,[61] L. J. Bel,[43] V. Bellee,[41] N. Belloli,[21,d] K. Belous,[37] I. Belyaev,[32] E. Ben-Haim,[8] G. Bencivenni,[19] S. Benson,[43] S. Beranek,[9] A. Berezhnoy,[33] R. Bernet,[42] A. Bertolin,[23] C. Betancourt,[42] F. Betti,[15] M.-O. Bettler,[40] M. van Beuzekom,[43] Ia. Bezshyiko,[42] S. Bifani,[47] P. Billoir,[8] A. Birnkraut,[10] A. Bitadze,[56] A. Bizzeti,[18,e] T. Blake,[50] F. Blanc,[41] J. Blouw,[11] S. Blusk,[61] V. Bocci,[26] T. Boettcher,[58] A. Bondar,[36,f] N. Bondar,[31] W. Bonivento,[16] I. Bordyuzhin,[32] A. Borgheresi,[21,d] S. Borghi,[56] M. Borisyak,[35] M. Borsato,[39] F. Bossu,[7] M. Boubdir,[9] T. J. V. Bowcock,[54] E. Bowen,[42] C. Bozzi,[17,40] S. Braun,[12] T. Britton,[61] J. Brodzicka,[56] E. Buchanan,[48] C. Burr,[56] A. Bursche,[16] J. Buytaert,[40] S. Cadeddu,[16] R. Calabrese,[17,a] M. Calvi,[21,d] M. Calvo Gomez,[38,g] A. Camboni,[38] P. Campana,[19] D. H. Campora Perez,[40] L. Capriotti,[56] A. Carbone,[15,h] G. Carboni,[25,i] R. Cardinale,[20,j] A. Cardini,[16] P. Carniti,[21,d] L. Carson,[52] K. Carvalho Akiba,[2] G. Casse,[54] L. Cassina,[21,d] L. Castillo Garcia,[41] M. Cattaneo,[40] G. Cavallero,[20] R. Cenci,[24,k] D. Chamont,[7] M. Charles,[8] Ph. Charpentier,[40] G. Chatzikonstantinidis,[47] M. Chefdeville,[4] S. Chen,[56] S. F. Cheung,[57] V. Chobanova,[39] M. Chrzaszcz,[42,27] A. Chubykin,[31] X. Cid Vidal,[39] G. Ciezarek,[43] P. E. L. Clarke,[52] M. Clemencic,[40] H. V. Cliff,[49] J. Closier,[40] V. Coco,[59] J. Cogan,[6] E. Cogneras,[5] V. Cogoni,[16,l] L. Cojocariu,[30] P. Collins,[40] A. Comerma-Montells,[12] A. Contu,[40] A. Cook,[48] G. Coombs,[40] S. Coquereau,[38] G. Corti,[40] M. Corvo,[17,a] C. M. Costa Sobral,[50] B. Couturier,[40] G. A. Cowan,[52] D. C. Craik,[52] A. Crocombe,[50] M. Cruz Torres,[62] S. Cunliffe,[55] R. Currie,[52] C. D'Ambrosio,[40] F. Da Cunha Marinho,[2] E. Dall'Occo,[43] J. Dalseno,[48] P. N. Y. David,[43] A. Davis,[3] K. De Bruyn,[6] S. De Capua,[56] M. De Cian,[12] J. M. De Miranda,[1] L. De Paula,[2] M. De Serio,[14,m] P. De Simone,[19] C. T. Dean,[53] D. Decamp,[4] M. Deckenhoff,[10] L. Del Buono,[8] H.-P. Dembinski,[11] M. Demmer,[10] A. Dendek,[28] D. Derkach,[35] O. Deschamps,[5] F. Dettori,[54] B. Dey,[22] A. Di Canto,[40] P. Di Nezza,[19] H. Dijkstra,[40] F. Dordei,[40] M. Dorigo,[41] A. Dosil Suárez,[39] A. Dovbnya,[45] K. Dreimanis,[54] L. Dufour,[43] G. Dujany,[56] K. Dungs,[40] P. Durante,[40] R. Dzhelyadin,[37] M. Dziewiecki,[12] A. Dziurda,[40] A. Dzyuba,[31] N. Déléage,[4] S. Easo,[51] M. Ebert,[52] U. Egede,[55] V. Egorychev,[32] S. Eidelman,[36,f] S. Eisenhardt,[52] U. Eitschberger,[10] R. Ekelhof,[10] L. Eklund,[53] S. Ely,[61] S. Esen,[12] H. M. Evans,[49] T. Evans,[57] A. Falabella,[15] N. Farley,[47] S. Farry,[54] R. Fay,[54] D. Fazzini,[21,d] D. Ferguson,[52] G. Fernandez,[38] A. Fernandez Prieto,[39] F. Ferrari,[15] F. Ferreira Rodrigues,[2] M. Ferro-Luzzi,[40] S. Filippov,[34] R. A. Fini,[14] M. Fiore,[17,a] M. Fiorini,[17,a] M. Firlej,[28] C. Fitzpatrick,[41] T. Fiutowski,[28] F. Fleuret,[7,n] K. Fohl,[40] M. Fontana,[16,40] F. Fontanelli,[20,j] D. C. Forshaw,[61] R. Forty,[40] V. Franco Lima,[54] M. Frank,[40] C. Frei,[40] J. Fu,[22,o] W. Funk,[40] E. Furfaro,[25,i] C. Färber,[40] A. Gallas Torreira,[39] D. Galli,[15,h] S. Gallorini,[23] S. Gambetta,[52] M. Gandelman,[2] P. Gandini,[57] Y. Gao,[3] L. M. Garcia Martin,[69] J. García Pardiñas,[39]

J. Garra Tico,[49] L. Garrido,[38] P. J. Garsed,[49] D. Gascon,[38] C. Gaspar,[40] L. Gavardi,[10] G. Gazzoni,[5] D. Gerick,[12] E. Gersabeck,[12] M. Gersabeck,[56] T. Gershon,[50] Ph. Ghez,[4] S. Gianì,[41] V. Gibson,[49] O. G. Girard,[41] L. Giubega,[30] K. Gizdov,[52] V. V. Gligorov,[8] D. Golubkov,[32] A. Golutvin,[55,40] A. Gomes,[1,p] I. V. Gorelov,[33] C. Gotti,[21,d] E. Govorkova,[43] R. Graciani Diaz,[38] L. A. Granado Cardoso,[40] E. Graugés,[38] E. Graverini,[42] G. Graziani,[18] A. Grecu,[30] R. Greim,[9] P. Griffith,[16] L. Grillo,[21,40,d] B. R. Gruberg Cazon,[57] O. Grünberg,[67] E. Gushchin,[34] Yu. Guz,[37] T. Gys,[40] C. Göbel,[62] T. Hadavizadeh,[57] C. Hadjivasiliou,[5] G. Haefeli,[41] C. Haen,[40] S. C. Haines,[49] B. Hamilton,[60] X. Han,[12] S. Hansmann-Menzemer,[12] N. Harnew,[57] S. T. Harnew,[48] J. Harrison,[56] M. Hatch,[40] J. He,[63] T. Head,[41] A. Heister,[9] K. Hennessy,[54] P. Henrard,[5] L. Henry,[69] E. van Herwijnen,[40] M. Heß,[67] A. Hicheur,[2] D. Hill,[57] C. Hombach,[56] P. H. Hopchev,[41] Z.-C. Huard,[59] W. Hulsbergen,[43] T. Humair,[55] M. Hushchyn,[35] D. Hutchcroft,[54] M. Idzik,[28] P. Ilten,[58] R. Jacobsson,[40] J. Jalocha,[57] E. Jans,[43] A. Jawahery,[60] F. Jiang,[3] M. John,[57] D. Johnson,[40] C. R. Jones,[49] C. Joram,[40] B. Jost,[40] N. Jurik,[57] S. Kandybei,[45] M. Karacson,[40] J. M. Kariuki,[48] S. Karodia,[53] M. Kecke,[12] M. Kelsey,[61] M. Kenzie,[49] T. Ketel,[44] E. Khairullin,[35] B. Khanji,[12] C. Khurewathanakul,[41] T. Kirn,[9] S. Klaver,[56] K. Klimaszewski,[29] T. Klimkovich,[11] S. Koliiev,[46] M. Kolpin,[12] I. Komarov,[41] R. Kopecna,[12] P. Koppenburg,[43] A. Kosmyntseva,[32] S. Kotriakhova,[31] A. Kozachuk,[33] M. Kozeiha,[5] L. Kravchuk,[34] M. Kreps,[50] P. Krokovny,[36,f] F. Kruse,[10] W. Krzemien,[29] W. Kucewicz,[27,c] M. Kucharczyk,[27] V. Kudryavtsev,[36,f] A. K. Kuonen,[41] K. Kurek,[29] T. Kvaratskheliya,[32,40] D. Lacarrere,[40] G. Lafferty,[56] A. Lai,[16] G. Lanfranchi,[19] C. Langenbruch,[9] T. Latham,[50] C. Lazzeroni,[47] R. Le Gac,[6] J. van Leerdam,[43] A. Leflat,[33,40] J. Lefrançois,[7] R. Lefèvre,[5] F. Lemaitre,[40] E. Lemos Cid,[39] O. Leroy,[6] T. Lesiak,[27] B. Leverington,[12] T. Li,[3] Y. Li,[7] Z. Li,[61] T. Likhomanenko,[35,68] R. Lindner,[40] F. Lionetto,[42] X. Liu,[3] D. Loh,[50] I. Longstaff,[53] J. H. Lopes,[2] D. Lucchesi,[23,q] M. Lucio Martinez,[39] H. Luo,[52] A. Lupato,[23] E. Luppi,[17,a] O. Lupton,[40] A. Lusiani,[24] X. Lyu,[63] F. Machefert,[7] F. Maciuc,[30] O. Maev,[31] K. Maguire,[56] S. Malde,[57] A. Malinin,[68] T. Maltsev,[36] G. Manca,[16,l] G. Mancinelli,[6] P. Manning,[61] J. Maratas,[5,r] J. F. Marchand,[4] U. Marconi,[15] C. Marin Benito,[38] M. Marinangeli,[41] P. Marino,[24,k] J. Marks,[12] G. Martellotti,[26] M. Martin,[6] M. Martinelli,[41] D. Martinez Santos,[39] F. Martinez Vidal,[69] D. Martins Tostes,[2] L. M. Massacrier,[7] A. Massafferri,[1] R. Matev,[40] A. Mathad,[50] Z. Mathe,[40] C. Matteuzzi,[21] A. Mauri,[42] E. Maurice,[7,n] B. Maurin,[41] A. Mazurov,[47] M. McCann,[55,40] A. McNab,[56] R. McNulty,[13] B. Meadows,[59] F. Meier,[10] D. Melnychuk,[29] M. Merk,[43] A. Merli,[22,40,o] E. Michielin,[23] D. A. Milanes,[66] M.-N. Minard,[4] D. S. Mitzel,[12] A. Mogini,[8] J. Molina Rodriguez,[1] I. A. Monroy,[66] S. Monteil,[5] M. Morandin,[23] M. J. Morello,[24,k] O. Morgunova,[68] J. Moron,[28] A. B. Morris,[52] R. Mountain,[61] F. Muheim,[52] M. Mulder,[43] M. Mussini,[15] D. Müller,[56] J. Müller,[10] K. Müller,[42] V. Müller,[10] P. Naik,[48] T. Nakada,[41] R. Nandakumar,[51] A. Nandi,[57] I. Nasteva,[2] M. Needham,[52] N. Neri,[22,40] S. Neubert,[12] N. Neufeld,[40] M. Neuner,[12] T. D. Nguyen,[41] C. Nguyen-Mau,[41,s] S. Nieswand,[9] R. Niet,[10] N. Nikitin,[33] T. Nikodem,[12] A. Nogay,[68] A. Novoselov,[37] D. P. O'Hanlon,[50] A. Oblakowska-Mucha,[28] V. Obraztsov,[37] S. Ogilvy,[19] R. Oldeman,[16,l] C. J. G. Onderwater,[70] J. M. Otalora Goicochea,[2] P. Owen,[42] A. Oyanguren,[69] P. R. Pais,[41] A. Palano,[14,m] M. Palutan,[19,40] A. Papanestis,[51] M. Pappagallo,[14,m] L. L. Pappalardo,[17,a] C. Pappenheimer,[59] W. Parker,[60] C. Parkes,[56] G. Passaleva,[18] A. Pastore,[14,m] M. Patel,[55] C. Patrignani,[15,h] A. Pearce,[40] A. Pellegrino,[43] G. Penso,[26] M. Pepe Altarelli,[40] S. Perazzini,[40] P. Perret,[5] L. Pescatore,[41] K. Petridis,[48] A. Petrolini,[20,j] A. Petrov,[68] M. Petruzzo,[22,o] E. Picatoste Olloqui,[38] B. Pietrzyk,[4] M. Pikies,[27] D. Pinci,[26] A. Pistone,[20] A. Piucci,[12] V. Placinta,[30] S. Playfer,[52] M. Plo Casasus,[39] T. Poikela,[40] F. Polci,[8] M. Poli Lener,[19] A. Poluektov,[50,36] I. Polyakov,[61] E. Polycarpo,[2] G. J. Pomery,[48] S. Ponce,[40] A. Popov,[37] D. Popov,[11,40] B. Popovici,[30] S. Poslavskii,[37] C. Potterat,[2] E. Price,[48] J. Prisciandaro,[39] C. Prouve,[48] V. Pugatch,[46] A. Puig Navarro,[42] G. Punzi,[24,t] C. Qian,[63] W. Qian,[50] R. Quagliani,[7,48] B. Rachwal,[28] J. H. Rademacker,[48] M. Rama,[24] M. Ramos Pernas,[39] M. S. Rangel,[2] I. Raniuk,[45] F. Ratnikov,[35] G. Raven,[44] F. Redi,[55] S. Reichert,[10] A. C. dos Reis,[1] C. Remon Alepuz,[69] V. Renaudin,[7] S. Ricciardi,[51] S. Richards,[48] M. Rihl,[40] K. Rinnert,[54] V. Rives Molina,[38] P. Robbe,[7] A. B. Rodrigues,[1] E. Rodrigues,[59] J. A. Rodriguez Lopez,[66] P. Rodriguez Perez,[56] A. Rogozhnikov,[35] S. Roiser,[40] A. Rollings,[57] V. Romanovskiy,[37] A. Romero Vidal,[39] J. W. Ronayne,[13] M. Rotondo,[19] M. S. Rudolph,[61] T. Ruf,[40] P. Ruiz Valls,[69] J. J. Saborido Silva,[39] E. Sadykhov,[32] N. Sagidova,[31] B. Saitta,[16,l] V. Salustino Guimaraes,[1] D. Sanchez Gonzalo,[38] C. Sanchez Mayordomo,[69] B. Sanmartin Sedes,[39] R. Santacesaria,[26] C. Santamarina Rios,[39] M. Santimaria,[19] E. Santovetti,[25,i] A. Sarti,[19,u] C. Satriano,[26,v] A. Satta,[25] D. M. Saunders,[48] D. Savrina,[32,33] S. Schael,[9] M. Schellenberg,[10] M. Schiller,[53] H. Schindler,[40] M. Schlupp,[10] M. Schmelling,[11] T. Schmelzer,[10] B. Schmidt,[40] O. Schneider,[41] A. Schopper,[40] H. F. Schreiner,[59] K. Schubert,[10] M. Schubiger,[41] M.-H. Schune,[7] R. Schwemmer,[40] B. Sciascia,[19] A. Sciubba,[26,u] A. Semennikov,[32] A. Sergi,[47] N. Serra,[42] J. Serrano,[6] L. Sestini,[23] P. Seyfert,[21] M. Shapkin,[37] I. Shapoval,[45] Y. Shcheglov,[31] T. Shears,[54] L. Shekhtman,[36,f] V. Shevchenko,[68] B. G. Siddi,[17,40] R. Silva Coutinho,[42] L. Silva de Oliveira,[2] G. Simi,[23,q] S. Simone,[14,m]

M. Sirendi,[49] N. Skidmore,[48] T. Skwarnicki,[61] E. Smith,[55] I. T. Smith,[52] J. Smith,[49] M. Smith,[55] l. Soares Lavra,[1] M. D. Sokoloff,[59] F. J. P. Soler,[53] B. Souza De Paula,[2] B. Spaan,[10] P. Spradlin,[53] S. Sridharan,[40] F. Stagni,[40] M. Stahl,[12] S. Stahl,[40] P. Stefko,[41] S. Stefkova,[55] O. Steinkamp,[42] S. Stemmle,[12] O. Stenyakin,[37] H. Stevens,[10] S. Stoica,[30] S. Stone,[61] B. Storaci,[42] S. Stracka,[24,t] M. E. Stramaglia,[41] M. Straticiuc,[30] U. Straumann,[42] L. Sun,[64] W. Sutcliffe,[55] K. Swientek,[28] V. Syropoulos,[44] M. Szczekowski,[29] T. Szumlak,[28] S. T'Jampens,[4] A. Tayduganov,[6] T. Tekampe,[10] G. Tellarini,[17,a] F. Teubert,[40] E. Thomas,[40] J. van Tilburg,[43] M. J. Tilley,[55] V. Tisserand,[4] M. Tobin,[41] S. Tolk,[49] L. Tomassetti,[17,a] D. Tonelli,[24] S. Topp-Joergensen,[57] F. Toriello,[61] R. Tourinho Jadallah Aoude,[1] E. Tournefier,[4] S. Tourneur,[41] K. Trabelsi,[41] M. Traill,[53] M. T. Tran,[41] M. Tresch,[42] A. Trisovic,[40] A. Tsaregorodtsev,[6] P. Tsopelas,[43] A. Tully,[49] N. Tuning,[43] A. Ukleja,[29] A. Ustyuzhanin,[35] U. Uwer,[12] C. Vacca,[16,l] V. Vagnoni,[15,40] A. Valassi,[40] S. Valat,[40] G. Valenti,[15] R. Vazquez Gomez,[19] P. Vazquez Regueiro,[39] S. Vecchi,[17] M. van Veghel,[43] J. J. Velthuis,[48] M. Veltri,[18,w] G. Veneziano,[57] A. Venkateswaran,[61] T. A. Verlage,[9] M. Vernet,[5] M. Vesterinen,[12] J. V. Viana Barbosa,[40] B. Viaud,[7] D. Vieira,[63] M. Vieites Diaz,[39] H. Viemann,[67] X. Vilasis-Cardona,[38,g] M. Vitti,[49] V. Volkov,[33] A. Vollhardt,[42] B. Voneki,[40] A. Vorobyev,[31] V. Vorobyev,[36,f] C. Voß,[9] J. A. de Vries,[43] C. Vázquez Sierra,[39] R. Waldi,[67] C. Wallace,[50] R. Wallace,[13] J. Walsh,[24] J. Wang,[61] D. R. Ward,[49] H. M. Wark,[54] N. K. Watson,[47] D. Websdale,[55] A. Weiden,[42] M. Whitehead,[40] J. Wicht,[50] G. Wilkinson,[57,40] M. Wilkinson,[61] M. Williams,[40] M. P. Williams,[47] M. Williams,[58] T. Williams,[47] F. F. Wilson,[51] J. Wimberley,[60] M. A. Winn,[7] J. Wishahi,[10] W. Wislicki,[29] M. Witek,[27] G. Wormser,[7] S. A. Wotton,[49] K. Wraight,[53] K. Wyllie,[40] Y. Xie,[65] Z. Xing,[61] Z. Xu,[4] Z. Yang,[3] Z. Yang,[60] Y. Yao,[61] H. Yin,[65] J. Yu,[65] X. Yuan,[36,f] O. Yushchenko,[37] K. A. Zarebski,[47] M. Zavertyaev,[11,b] L. Zhang,[3] Y. Zhang,[7] A. Zhelezov,[12] Y. Zheng,[63] X. Zhu,[3] V. Zhukov,[33] and S. Zucchelli[15]

(LHCb Collaboration)

[1]*Centro Brasileiro de Pesquisas Físicas (CBPF), Rio de Janeiro, Brazil*
[2]*Universidade Federal do Rio de Janeiro (UFRJ), Rio de Janeiro, Brazil*
[3]*Center for High Energy Physics, Tsinghua University, Beijing, China*
[4]*LAPP, Université Savoie Mont-Blanc, CNRS/IN2P3, Annecy-Le-Vieux, France*
[5]*Clermont Université, Université Blaise Pascal, CNRS/IN2P3, LPC, Clermont-Ferrand, France*
[6]*CPPM, Aix-Marseille Université, CNRS/IN2P3, Marseille, France*
[7]*LAL, Université Paris-Sud, CNRS/IN2P3, Orsay, France*
[8]*LPNHE, Université Pierre et Marie Curie, Université Paris Diderot, CNRS/IN2P3, Paris, France*
[9]*I. Physikalisches Institut, RWTH Aachen University, Aachen, Germany*
[10]*Fakultät Physik, Technische Universität Dortmund, Dortmund, Germany*
[11]*Max-Planck-Institut für Kernphysik (MPIK), Heidelberg, Germany*
[12]*Physikalisches Institut, Ruprecht-Karls-Universität Heidelberg, Heidelberg, Germany*
[13]*School of Physics, University College Dublin, Dublin, Ireland*
[14]*Sezione INFN di Bari, Bari, Italy*
[15]*Sezione INFN di Bologna, Bologna, Italy*
[16]*Sezione INFN di Cagliari, Cagliari, Italy*
[17]*Sezione INFN di Ferrara, Ferrara, Italy*
[18]*Sezione INFN di Firenze, Firenze, Italy*
[19]*Laboratori Nazionali dell'INFN di Frascati, Frascati, Italy*
[20]*Sezione INFN di Genova, Genova, Italy*
[21]*Sezione INFN di Milano Bicocca, Milano, Italy*
[22]*Sezione INFN di Milano, Milano, Italy*
[23]*Sezione INFN di Padova, Padova, Italy*
[24]*Sezione INFN di Pisa, Pisa, Italy*
[25]*Sezione INFN di Roma Tor Vergata, Roma, Italy*
[26]*Sezione INFN di Roma La Sapienza, Roma, Italy*
[27]*Henryk Niewodniczanski Institute of Nuclear Physics Polish Academy of Sciences, Kraków, Poland*
[28]*AGH - University of Science and Technology, Faculty of Physics and Applied Computer Science, Kraków, Poland*
[29]*National Center for Nuclear Research (NCBJ), Warsaw, Poland*
[30]*Horia Hulubei National Institute of Physics and Nuclear Engineering, Bucharest-Magurele, Romania*
[31]*Petersburg Nuclear Physics Institute (PNPI), Gatchina, Russia*
[32]*Institute of Theoretical and Experimental Physics (ITEP), Moscow, Russia*
[33]*Institute of Nuclear Physics, Moscow State University (SINP MSU), Moscow, Russia*

[34]Institute for Nuclear Research of the Russian Academy of Sciences (INR RAN), Moscow, Russia
[35]Yandex School of Data Analysis, Moscow, Russia
[36]Budker Institute of Nuclear Physics (SB RAS), Novosibirsk, Russia
[37]Institute for High Energy Physics (IHEP), Protvino, Russia
[38]ICCUB, Universitat de Barcelona, Barcelona, Spain
[39]Universidad de Santiago de Compostela, Santiago de Compostela, Spain
[40]European Organization for Nuclear Research (CERN), Geneva, Switzerland
[41]Institute of Physics, Ecole Polytechnique Fédérale de Lausanne (EPFL), Lausanne, Switzerland
[42]Physik-Institut, Universität Zürich, Zürich, Switzerland
[43]Nikhef National Institute for Subatomic Physics, Amsterdam, The Netherlands
[44]Nikhef National Institute for Subatomic Physics and VU University Amsterdam, Amsterdam, The Netherlands
[45]NSC Kharkiv Institute of Physics and Technology (NSC KIPT), Kharkiv, Ukraine
[46]Institute for Nuclear Research of the National Academy of Sciences (KINR), Kyiv, Ukraine
[47]University of Birmingham, Birmingham, United Kingdom
[48]H.H. Wills Physics Laboratory, University of Bristol, Bristol, United Kingdom
[49]Cavendish Laboratory, University of Cambridge, Cambridge, United Kingdom
[50]Department of Physics, University of Warwick, Coventry, United Kingdom
[51]STFC Rutherford Appleton Laboratory, Didcot, United Kingdom
[52]School of Physics and Astronomy, University of Edinburgh, Edinburgh, United Kingdom
[53]School of Physics and Astronomy, University of Glasgow, Glasgow, United Kingdom
[54]Oliver Lodge Laboratory, University of Liverpool, Liverpool, United Kingdom
[55]Imperial College London, London, United Kingdom
[56]School of Physics and Astronomy, University of Manchester, Manchester, United Kingdom
[57]Department of Physics, University of Oxford, Oxford, United Kingdom
[58]Massachusetts Institute of Technology, Cambridge, Massachusetts, USA
[59]University of Cincinnati, Cincinnati, Ohio, USA
[60]University of Maryland, College Park, Maryland, USA
[61]Syracuse University, Syracuse, New York, USA
[62]Pontifícia Universidade Católica do Rio de Janeiro (PUC-Rio), Rio de Janeiro, Brazil (associated with Institution Universidade Federal do Rio de Janeiro (UFRJ), Rio de Janeiro, Brazil)
[63]University of Chinese Academy of Sciences, Beijing, China (associated with Institution Center for High Energy Physics, Tsinghua University, Beijing, China)
[64]School of Physics and Technology, Wuhan University, Wuhan, China (associated with Institution Center for High Energy Physics, Tsinghua University, Beijing, China)
[65]Institute of Particle Physics, Central China Normal University, Wuhan, Hubei, China (associated with Institution Center for High Energy Physics, Tsinghua University, Beijing, China)
[66]Departamento de Fisica, Universidad Nacional de Colombia, Bogota, Colombia (associated with Institution LPNHE, Université Pierre et Marie Curie, Université Paris Diderot, CNRS/IN2P3, Paris, France)
[67]Institut für Physik, Universität Rostock, Rostock, Germany (associated with Institution Physikalisches Institut, Ruprecht-Karls-Universität Heidelberg, Heidelberg, Germany)
[68]National Research Centre Kurchatov Institute, Moscow, Russia (associated with Institution Institute of Theoretical and Experimental Physics (ITEP), Moscow, Russia)
[69]Instituto de Fisica Corpuscular, Centro Mixto Universidad de Valencia - CSIC, Valencia, Spain (associated with Institution ICCUB, Universitat de Barcelona, Barcelona, Spain)
[70]Van Swinderen Institute, University of Groningen, Groningen, The Netherlands (associated with Institution Nikhef National Institute for Subatomic Physics, Amsterdam, The Netherlands)

[a]Also at Università di Ferrara, Ferrara, Italy.
[b]Also at P.N. Lebedev Physical Institute, Russian Academy of Science (LPI RAS), Moscow, Russia.
[c]Also at AGH - University of Science and Technology, Faculty of Computer Science, Electronics and Telecommunications, Kraków, Poland.
[d]Also at Università di Milano Bicocca, Milano, Italy.
[e]Also at Università di Modena e Reggio Emilia, Modena, Italy.
[f]Also at Novosibirsk State University, Novosibirsk, Russia.
[g]Also at LIFAELS, La Salle, Universitat Ramon Llull, Barcelona, Spain.
[h]Also at Università di Bologna, Bologna, Italy.
[i]Also at Università di Roma Tor Vergata, Roma, Italy.
[j]Also at Università di Genova, Genova, Italy.
[k]Also at Scuola Normale Superiore, Pisa, Italy.
[l]Also at Università di Cagliari, Cagliari, Italy.

[m]Also at Università di Bari, Bari, Italy.
[n]Also at Laboratoire Leprince-Ringuet, Palaiseau, France.
[o]Also at Università degli Studi di Milano, Milano, Italy.
[p]Also at Universidade Federal do Triângulo Mineiro (UFTM), Uberaba-MG, Brazil.
[q]Also at Università di Padova, Padova, Italy.
[r]Also at Iligan Institute of Technology (IIT), Iligan, Philippines.
[s]Also at Hanoi University of Science, Hanoi, Viet Nam.
[t]Also at Università di Pisa, Pisa, Italy.
[u]Also at Università di Roma La Sapienza, Roma, Italy.
[v]Also at Università della Basilicata, Potenza, Italy.
[w]Also at Università di Urbino, Urbino, Italy.